The influence of electron emission on heat load to the plasma facing materials under space charge limited condition with an oblique magnetic field

I.V. Tsvetkov [1], T. Tanabe [*]

Center for Integrated Research in Science and Engineering, Nagoya University, Furo-cho, Chikusaku, Nagoya 464-8603, Japan

Abstract

The effect of electron emission on the potential distribution in the sheath and heat load on divertor plates has been studied taking into account the occurrence of space charge limited conditions (SCLC) and its extreme case of a virtual cathode under the existence of an oblique magnetic field. Interactions among heat flux from plasma, surface temperature, and thermo-electron emission are simulated considering self-consistency among electron transport, deposited heat and material thermal response for Be, C, Mo and W under the condition of plasma temperature $T_e = 40$ eV, plasma density $n_0 = 10^{19}$ m^{-3} and magnetic field strength $B = 2$ T with an angle between magnetic field and surface $\alpha = 10°$. At lower surface temperatures, secondary electron emission dominates the total electron emission, whereas thermo-electron emission is superior at high surface temperatures. Both are promptly returned to the surface by an oblique magnetic field but the effect is more significant on the secondary electrons. In order to attain the SCLC condition, a substantial amount of thermo-electron emission (and hence higher surface temperature) is required. Heat flux from plasma and the surface temperature increase with time due to the increase of total electron emission. However, once SCLC is attained, the heat flux tends to saturate at a certain temperature. For C and W, with the aid of an oblique magnetic field, the SCLC condition is very likely maintained and consequently W surface would be free from the melting. Be and Mo, on the other hand, the amount of emitted electrons does not seem enough to maintain the SCLC and their surface temperature should be elevated. © 1999 Elsevier Science B.V. All rights reserved.

Keywords: Electrons; Secondary electron; Sheath potential; Space charge limitation; Surface temperature response; SOL modelling

1. Introduction

In order to avoid significant erosion of low Z materials, large part of divertor is designed to be covered by high Z materials such as Mo and W in ITER like burning plasma machines [1]. It is well known that electron emission from material surfaces plays a very important role in the plasma–surface interaction and influences the boundary plasma accordingly. Electron emission characteristics of high Z materials are quite different from that of low Z materials i.e., larger secondary emission coefficients, higher average energy in energy distribution of the secondary electrons, larger reflection coefficients and so on. Such differences in the electron emission characteristics among the materials should have certain influence on the boundary plasma. Basically a large amount of the electron emission is expected to reduce the sheath potential. This should result in the reduction of both the ion energy flux to the surface and the sputtering yield. Several tokamaks have started to investigate the high Z impurity behavior in their plasma and found that the plasma tolerates the

---
[*] Corresponding author. Tel.: +81 52 789 5177; e-mail: tanabe@cirse.nagoya-u.ac.jp
[1] Permanent affiliation: Department of Plasma Physics, Moscow Engineering Physics Institute, 115409 Moscow, Russian Federation. E-mail: tsvetkov@plasm.mephi.msk.su

high Z wall owing to the prompt return of sputtered impurities by their gyromotion after ionization in an oblique magnetic field [2]. At the same time electron flux to the target should be enhanced. As a result, a local hot spot would be produced on the materials surface emitting large amounts of thermal electrons. Accordingly a virtual cathode would be formed just in front of the surface. However, no systematic investigation on the electron emission has been, in our knowledge, done until now, except some simulation experiments [3–5].

Recently we have made a computer simulation on the reduction of the effective secondary yields $\delta_e(E_p)$ (the number of secondary electrons passing through the sheath from the wall surface per primary electron with incident energy E_p) in the space charge limited condition (SCLC) by the prompt return of the secondary electrons caused by their gyromotion in the oblique magnetic field [6]. The absolute number of the secondary electron emission coefficient γ_e ($\gamma_e = \int \delta_e(E_p)f(E_p)\,dE_p / \int f(E_p)\,dE_p$; the number of electrons returning to the boundary plasma per primary electron with an incident energy distribution $f(E_p)$) in SCLC has been presented in Ref. [7]. However, the self-consistence among the electron emission on heat load and material thermal response in an oblique magnetic field has not been examined.

In the present work, the influence of the electron emission on the potential distribution in the sheath and the heat load on the divertor plate has been studied taking into account the occurrence of SCLC and a virtual cathode. The interaction between heat flux from the plasma and thermo-electron emitting surface is simulated considering self-consistency among electron transport in the sheath including primary-, secondary- and thermo-electrons, deposited heat and material thermal response for Be, C, Mo and W as target materials. Fig. 1 schematically illustrates all phenomena considered here. Two quite different conditions of the magnetic field, i.e., with and without an oblique magnetic field are compared taking into account the occurrence of a virtual cathode.

2. Model

2.1. The potential distribution in the sheath

To describe the potential distribution $\varphi(x)$ in the plasma sheath considering the occurrence of a virtual cathode near surface, we have modified Poisson's equation given in Ref. [6] by adding a parameter ε_e for the initial energy of emitted electrons as
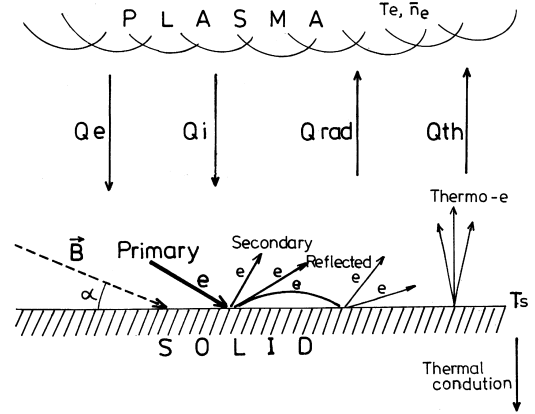

Fig. 1. Schematic illustration for all interactions considered in the present simulation. Q_e, Q_e, Q_{rad}, and Q_{th} represent electron heat flux, ion heat flux, radiative losses and heat flux carried by thermo-electrons, respectively. The total heat flux Q_{tot} is defined as $Q_{tot} = Q_e + Q_i - Q_{rad} - Q_{th}$.

$$\frac{d^2\chi}{d\xi^2} = -\frac{1}{\sqrt{1 - \frac{\chi}{\varepsilon_i}}} + \left(1 - \frac{\gamma}{1-\gamma}\sqrt{\frac{m_e \varepsilon_i}{m_i(-\chi_s + \varepsilon_e)}}\right)\exp(\chi)$$
$$+ \frac{\gamma}{1-\gamma}\sqrt{\frac{m_e \varepsilon_i}{m_i(\chi - \chi_s + \varepsilon_e)}}, \qquad (1)$$

where $\chi = e\varphi/kT_e$ is the normalized potential; T_e the plasma temperature; $\chi_s = e\varphi_s/kT_e$, normalized sheath potential; $\xi = x/\lambda_D$, normalized distance; $\lambda_D = (\varepsilon_0 kT_e/n_0 e^2)^{1/2}$, Debye length; $\varepsilon_I = v_{0i}^2 m_i/2kT_e$, v_{0i} is the mean ion velocity in the x-direction at the sheath edge; $\varepsilon_e = v_{0e}^2 m_e/2kT_e$, v_{0e} is the mean velocity of electrons emitted from the surface.

The effective emission coefficient γ is defined as the function of an effective electron emission coefficient Γ_e and an angle α between the magnetic field and the target surface (Fig. 1):

$$\gamma = \frac{\Gamma_e}{\sin\alpha + \Gamma_e(1 - \sin\alpha)}. \qquad (2)$$

The effective electron emission coefficient

$$\Gamma_e = \frac{\gamma_e + \gamma_t}{1 + \gamma_t} \qquad (3)$$

includes secondary electron emission coefficient γ_e and thermo-electron emission coefficient $\gamma_t = k_t\gamma_j$. The reducing factor k_t represents the suppression of the thermo-electron emission by the negative electric field of the virtual cathode and the gyration in an oblique magnetic field. We define the coefficient of the thermo-electron emission in ordinary regime as $\gamma_j = j_t/en_0v_{0i}$, where j_t is thermo-ionic current, and n_0v_{0i} as the average ion flux impinging to the surface. It should be noted that the effective emission coefficient γ is dependent both on the

secondary and thermo-electron emissions and on the magnetic field angle α, because the oblique magnetic field suppresses the emission flux in the sheath and increases electron density near the surface. The self-consistent solution of Eq. (1) determines the potential distribution $\varphi(x)$ in the sheath as a function of γ as already described in Ref. [7].

When γ exceeds the critical value of 0.905, a virtual cathode is eventually formed in front of the surface, where the electric field becomes negative as shown in Fig. 2. One should note that such a virtual cathode with the negative electric field is not stable. Because some

parts of the electrons emitted from the surface are reflected back to the surface by the negative potential hill of the virtual cathode, which, consequently, makes the electric field on the surface return to zero (SCLC). The height $\Delta\varphi$ and location x_h of the negative potential hill are dependent on the initial energy of the emitted electrons ε_e.

2.2. Electron emission

For the calculation, basic data of secondary electron emission coefficients, reflection coefficients and energy distribution of emitted electrons for Be, C, Mo and W are the same as in Ref. [6]. Maxwellian velocity distributions are assumed both for primary electrons and thermo-electrons. The modified Possion's Eq. (1) in the sheath was solved numerically by the Runge–Kutta method with an integration step automatically chosen to ensure an error less than $10^{-4}\lambda_D$. Simple mirror reflection was assumed for the energy and angular distributions of reflected electrons but their amount was reduced by the reflection coefficient. When the reflected electrons are promptly returned to the surface due to their gyration, some of them are subsequently reflected or produce secondary electrons depending on their energy (Fig. 1). Calculations were made for 1 million primary electrons having the Maxwellian velocity distribution modified by the sheath potential with a velocity component v_x normal to the surface

$$dN(v_x) = (m_e n_0/kT_e)\exp(-m_e v_x^2/2kT_e)v_x\,dv_x. \quad (4)$$

Since the thickness of the sheath could not be determined exactly, we took $d = 5\lambda_D$ to take into account the effects of high energy electrons. We have made additional calculations changing d from $d = \lambda_D$ to $d = 10\lambda_D$, and found that the results were not significantly altered.

The thermo-electron emission or current density j_t changes with surface temperature T_s and work function φ_a of materials as represented by the Richardson–Dushman equation

$$j_t = AT_s^2\exp(-\varphi_a/kT_s). \quad (5)$$

The temperature dependences of both Dushman's constant A and work function φ_a are given in Ref. [8] based on the experimental data for C, Mo, W in Refs. [9,10]. Thermo-electron emission becomes appreciable at temperatures above 2000 K. Therefore, the thermo-electron emission from Be having melting point at 1553 K is not discussed in detail.

In an oblique magnetic field, some of the thermo-electrons return to the surface by gyration. The reducing coefficient k_t (the number of electrons passing through the sheath per emitted electrons) was calculated for different potential distributions by means of a transport
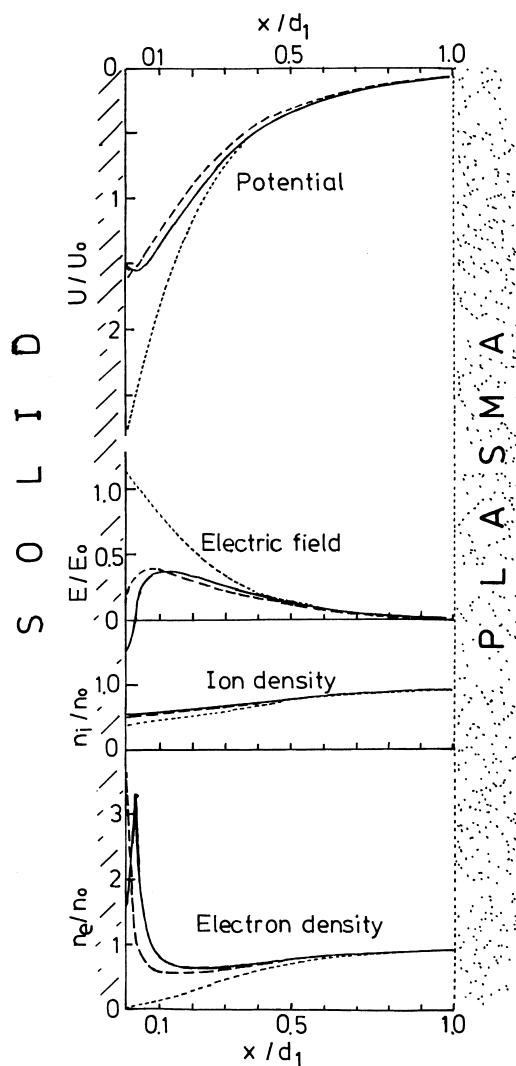

Fig. 2. Potential, electric field, ion and electron distributions in the sheath; dotted lines for ordinary regime ($\gamma = 0$), broken lines for the space–charge limitation ($\gamma = 0.905$ and $\varepsilon_e = 0$) and solid lines for a virtual cathode regime ($\gamma = 0.91$ and $\varepsilon_e = 0.05$), $E_0 = kT_e/e\lambda_D$.

simulation of the thermo-electrons in the sheath. The thermo-electrons are assumed to have a Maxwellian velocity distribution with a velocity component v_x normal to the surface.

$$dN(v_x) = (m_e N/kT_s) \exp(-m_e v_x^2/2kT_s)v_x \, dv_x, \qquad (6)$$

where $N = j_t/e$ and $\cos(\theta)$ dependence of the emission angles (the angle θ is respected to a surface normal). In SCLC, k_t decreases to the value of 0.67 owing to the prompt return of the thermo-electrons by gyration.

Fig. 3(a) shows the effective electron emission coefficient Γ_e as a function of surface temperature T_s with various values of γ for W under the condition of the plasma temperature $T_e = 40$ eV, and the plasma density $n_0 = 10^{19}$ m^{-3}, the angle between the magnetic field and the target surface $\alpha = 10°$. The dependence of Γ_e on γ is remarkable only for lower surface temperatures T_s, because for low T_s the effective electron emission coefficient is dominated by secondary electrons, which are strongly suppressed by the magnetic field (by a factor of more than 3), whereas at higher T_s, Γ_e is dominated by the thermo-electron emission, for which prompt return is not so significant (only a factor of 1.5 or less)

owing to their smaller energy. Fig. 3(b) shows the effect of the angle α between the magnetic field and the target surface on the relation between Γ_e vs. T_s. As seen in the figure the significant reduction of Γ_e becomes appreciable for α less than 20°. As already demonstrated in Ref. [6], the dependence of γ on α is not monotonic. With decreasing α from 90° to 10°, γ increases according to the change in the magnetic field strength itself (emitted flux suppression by magnetic field or increase of electron density near the surface). Below 10°, γ is reduced by the prompt return of the emitted electrons. In the following calculations we, therefore, fixed α at 10° with magnetic field $B = 2$ T, plasma temperature $T_e = 40$ eV, and plasma density $n_0 = 10^{19}$ m^{-3}.

2.3. Material thermal response

The thermal response of the plasma facing materials is calculated by solving a time-dependent heat conduction equation. For simplicity, one-dimensional heat flow in the materials (with the infinite thickness) is assumed as given by

$$\rho c_p \frac{\partial T}{\partial t} = \frac{\partial}{\partial x}\left(k\frac{\partial T}{\partial x}\right), \qquad (7)$$

where x is the direction perpendicular to the surface, ρ the density, c_p the specific heat, and k the thermal conductivity. The temperature dependence of the thermophysical properties are approximated by suitable analytical equations [11–16]. The time evolution of the surface temperature can be given by the boundary conditions as

$$-k\frac{\partial T}{\partial x}(0,t) = Q_{tot}. \qquad (8)$$

The total heat flux Q_{tot} includes the electron heat flux Q_e and the ion heat flux Q_i from plasma, the radiative losses Q_{rad} and the heat flux taken by thermo-electrons Q_{th} from the material surface:

$$Q_{tot} = Q_e + Q_i - Q_{rad} - Q_{th}. \qquad (9)$$

The plasma heat flux to the target is determined mainly by the kinetic energy associated with impinging plasma particles:

$$Q_e + Q_i = \left(\frac{2k_B T_e}{1-\gamma} + \frac{k_B T_e}{2} + e\varphi_s\right)n_0\sqrt{\frac{k_B T_e}{m_i}}\sin\alpha. \qquad (10)$$

This heat flux decreases as $\sin\alpha$ with decreasing magnetic field angle α. For the radiative losses from the surface we assumed Stefan–Boltzmann law

$$Q_{rad} = \sigma\varepsilon T^4, \qquad (11)$$

where σ is the Stefan–Boltzmann constant, and as the emissivity ε is $\varepsilon = 0.2$ for Be and Mo, $\varepsilon = 0.5$ for C,
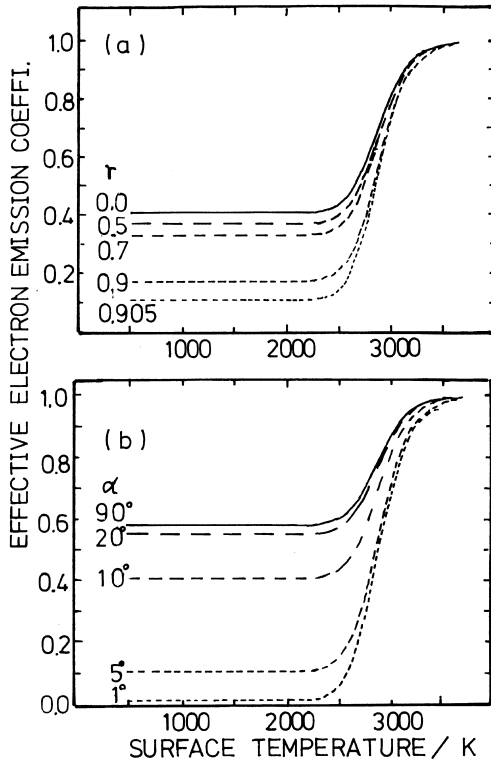

Fig. 3. Surface temperature dependence of effective electron emission coefficient $\Gamma_e = (\gamma_e + \gamma_t)/(1 + \gamma_t)$ for W on (a) various effective emission coefficient γ and (b) various angle α between magnetic field and surface ($T_e = 40$ eV, $n_0 = 10^{19}$ m^{-3}).

$\varepsilon = 0.4$ for W [14]. The heat loss due to thermo-electron emission can be given by

$$Q_{th} = (\varphi_a + 2k_B T_s/e) k_t j_{th} \sin \alpha. \tag{12}$$

Using the dependence of potential distribution in the sheath and heat fluxes on G_e and γ, we have determined the time-dependent quantities self-consistently by an iterative process in each time step.

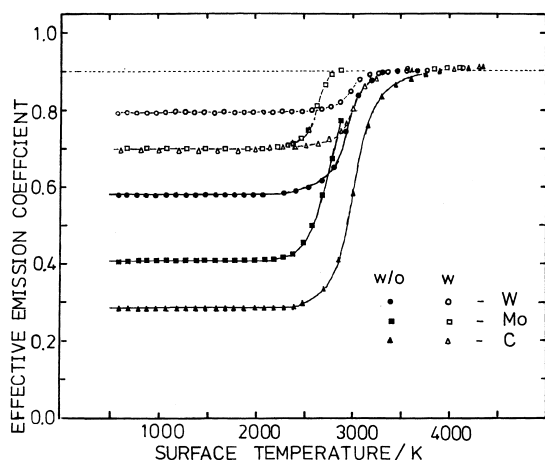## 3. Results of self-consistent analysis

Fig. 4 shows the self-consistent effective emission coefficient γ for C, Mo, and W as a function of the surface temperature T_s, with and without an oblique magnetic field. The increase of γ above 2500 K in all materials is mainly due to the thermo-electron emission. The figure clearly indicates that the effect of the magnetic field, with which γ exceeds the critical value of 0.905 at lower surface temperature compared to that without magnetic field or with magnetic field perpendicular to the surface. For example, in case with the magnetic field the surface temperature of Mo reaches melting point (2900 K) for $\gamma = 0.76$ instead of $\gamma = 0.9$ without the magnetic field.

As shown in Fig. 5, the responses of heat fluxes to surface temperature through the effective emission coefficient γ, are also quite different between the two cases. In general, the electron heat flux, Q_e, increases with γ, whereas the ion heat flux, Q_i, decreases because the sheath potential φ_s decreases. The radiation, Q_{rad}, and the heat removal by thermo-electrons, Q_{th}, increase with

Fig. 5. Self-consistent effective emission coefficient γ for W and heat fluxes as a function of the surface temperature T_s for (a) without and (b) with an oblique magnetic field ($B = 2$ T, $\alpha = 10°$, $T_e = 40$ eV, $n_0 = 10^{19}$ m^{-3}).

T_s. However, the reduction of the total heat flux with the oblique magnetic field is significant, i.e., six times smaller than that without the magnetic field or with the magnetic field perpendicular to the surface. In addition, in SCLC with the oblique magnetic field, the total heat flux Q_{tot} saturates at a certain temperature and decreases at higher temperatures due to the decrease of γ, consequently the SCLC condition is maintained (Fig. 5). Be, C and Mo show very similar results. Time dependence of the total heat flux and surface temperature are illustrated in Fig. 6. The heat flux from plasma, the dominant part of which is brought by incident electrons, and the surface temperature increase with time because of the increase of γ. One can see, the incubation time for surface-temperature escalation is far longer with the oblique magnetic field than that without the magnetic field for all materials (Be, C, Mo, W). Without the oblique magnetic field, only C shall suffer the occurrence of SCLC without surface melting, and all others (Be, Mo and W) will be melted without attaining the SCLC conditions. The oblique magnetic field, on the other hand, suppresses electron emission and leads to SCLC.

Fig. 4. Self-consistent effective emission coefficient γ for C, Mo, and W as a function of the surface temperature T_s with and without an oblique magnetic field (magnetic field strength $B = 2$ T, angle between magnetic field and surface $\alpha = 10°$, plasma temperature $T_e = 40$ eV, plasma density $n_0 = 10^{19}$ m^{-3}).

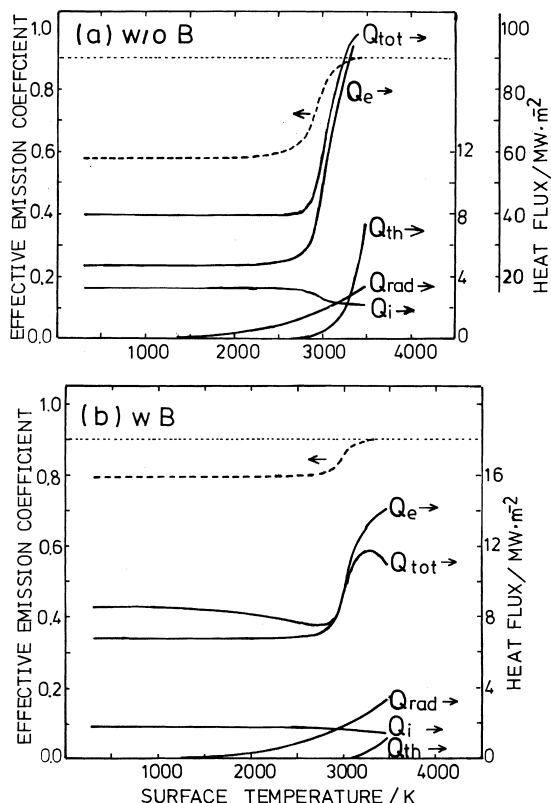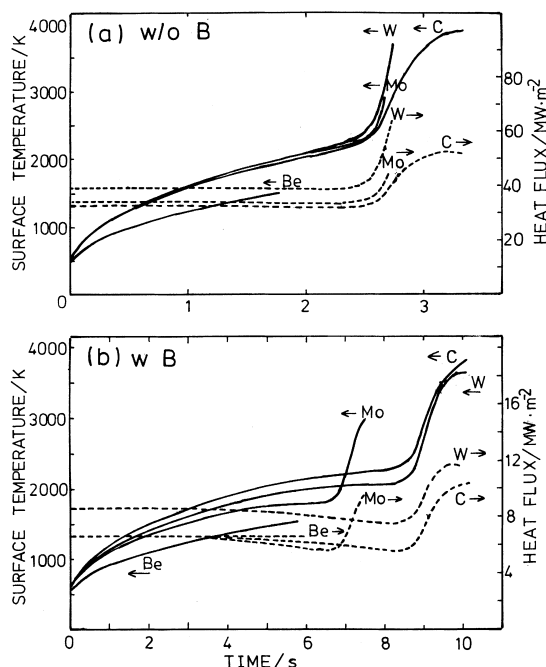Fig. 6. Surface temperature T_s and total heat fluxes for Be, C, Mo and W as a function of time (a) without and (b) with an oblique magnetic field ($B = 2$ T, $\alpha = 10°$, $T_e = 40$ eV, $n_0 = 10^{19}$ m^{-3}).

Thus, the surface of C and W will be sustained without melting in SCLC. But Be and Mo cannot produce enough amount of emitted electrons to attain SCLC and would melt.

For simplicity we assumed that the plasma temperature and density at the sheath are not influenced by the electron emission. We believe the present results are not so much different from the realistic solution. Nevertheless, development of more realistic self-consistent model including the behavior of ions is necessary.

4. Conclusions

The present work is devoted to the simulation of the interaction between heat flux from plasma and consequently emitted thermo-electrons from the surface under the existence of an oblique magnetic field, taking into account the self-consistency among electron transport in the sheath, deposited heat and material thermal response for Be, C, Mo and W as the target materials.

Generally, a large amount of electron emission results in the SCLC condition and hence the heat load from plasma can be reduced. For low surface temperatures, secondary electron emission dominates the total electron emission, whereas for high surface temperatures thermo-electron emission is superior. Both are promptly

returned to the surface by an oblique magnetic field and the effect is more significant on the secondary electron emission. Therefore the SCLC condition is not likely caused solely by the secondary electron emission but thermo-electron emission (and hence higher surface temperature) seems indispensable. At very high temperatures, a virtual cathode would be eventually formed but is not stable.

The heat flux from the plasma, the dominant part of which is brought by incident electrons, and surface temperature increases with time because of the increase of the effective electron emission coefficient γ. With increasing surface temperature thermo-electron emission becomes dominant, resulting SCLC with the aid of the oblique magnetic field. Without the oblique magnetic field, only C shall be subjected to the SCLC condition, and all others (Be, Mo and W) will melt before the attaining the SCLC conditions. Under the oblique magnetic field, W will sustain the SCLC condition without melting. But Be and Mo cannot produce enough amount of emitted electrons to attain SCLC and would melt down easily.

References

[1] R. Parker et al., Nucl. Fusion 241–243 (1997) 1.
[2] K. Ohya, J. Kawata, T. Tanabe et al., Proceedings of the 1996 International Conference on Plasma Physics, Nagoya, 1996, p. 650.
[3] M.Y. Ye, S. Takamura, N. Ohno, J. Nucl. Mater. 241–243 (1997) 1243.
[4] V. Rohde, M. Laux, P. Bachmann et al., J. Nucl. Mater. 241–243 (1997) 712.
[5] R. Choudra, in: D.E. Post, R. Behrisch (Eds.), Physics of Plasma–Wall Interactions in Controlled Fusion, Plenum, New York, 1986, pp. 99–134.
[6] I.V. Tsvetkov, T. Tanabe, J. Nucl. Mater. 258–263 (1998) 927.
[7] I.V. Tsvetkov, T. Tanabe, The secondary electron emission coefficient in the space charge limited condition with an oblique magnetic field, Nucl. Fusion, submitted.
[8] R.M. Rose, L.A. Shepard, J. Wulf, Electronic properties, The Structure and Properties of Materials, vol. IV, Wiley, New York, 1966, p. 34.
[9] K. Ertl, R.Behrish, Physics of Plasma–Wall Interaction in Controlled Fusion, Plenum, New York, 1986, p. 515.
[10] T. Tanabe, Suppl. J. Nucl. Fusion 5 (1994) 129.
[11] O. Kubaschewski, C.B. Alcock, P.J. Spencer, Materials Thermo-chemistry, Pergamon, Oxford, 1993, p. 257.

720 I.V. Tsvetkov, T. Tanabe / Journal of Nuclear Materials 266–269 (1999) 714–720

[12] CRC Handbook of Chemistry and Physics, CRC, New York, 1997.

[13] Proceedings of ITER JOINT WORK JAERI, Specialist Meeting on Material Data Base Plasma Facing Materials, 7–9 February 1990, pp. 39–41.

[14] J.P. Holman, Heat Transfer, 4th ed., McGrawhill, 1972.

[15] Smithells, Metals Reference Book, Butterworths, London, 1949.

[16] Proceedings of ITER JOINT WORK JAERI, Specialist Meeting on Material Data Base on Plasma Fasing Materials, 7–9 February 1990, p. 62.